

1

Supplementary information for

2

Age-dependent decline in stress response capacity revealed by

3

proteins dynamics analysis

4

Kaiyue Chen^{1,2}, Wenting Shen², Zhiwen Zhang¹, Fangzheng Xiong¹, Qi Ouyang^{1,2,3}, Chunxiong

5

Luo^{1,2*}

6

¹The State Key Laboratory for Artificial Microstructures and Mesoscopic Physics, School of

7

Physics, Peking University, China. ²Center for Quantitative Biology, Academy for Advanced

8

Interdisciplinary Studies, Peking University, China. ³Peking-Tsinghua Center for Life Sciences,

9

Peking University, Beijing, China.

10

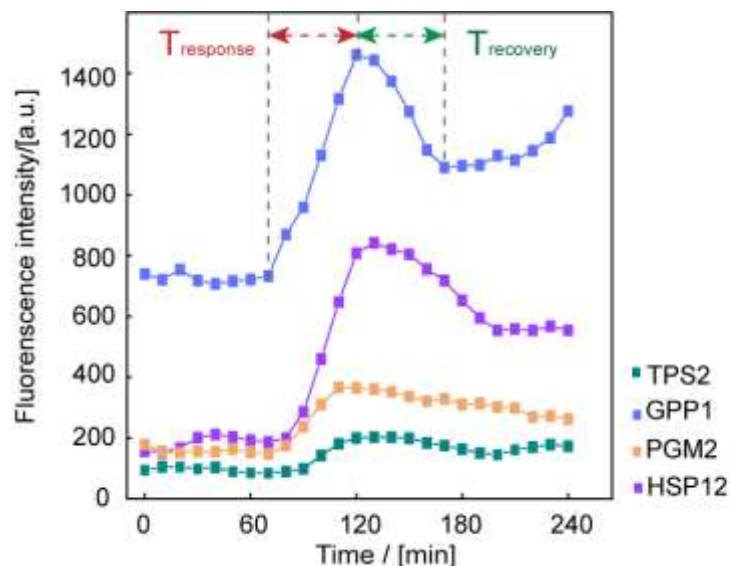
*To whom correspondence should be addressed: Chunxiong Luo, email: pkuluocx@pku.edu.cn

11

12

Supplementary Figures

13



14

15

16

Supplementary Figure 1. Recovery times of yeasts under stimulation with sustained hyperosmotic pressure (0.4 M KCl).

17

18

To estimate the response and adaptation time of cells to osmotic stress, we added continuous

19

osmotic pressure (0.4 M KCl) stimulation at 80 min. The response time is the time it takes for the

20

base value to reach the fluorescence maximum. Recovery time is adapted from the maximum to

21

the constant value. The response time and recovery time were approximately 1 h and 2~3 h,

22

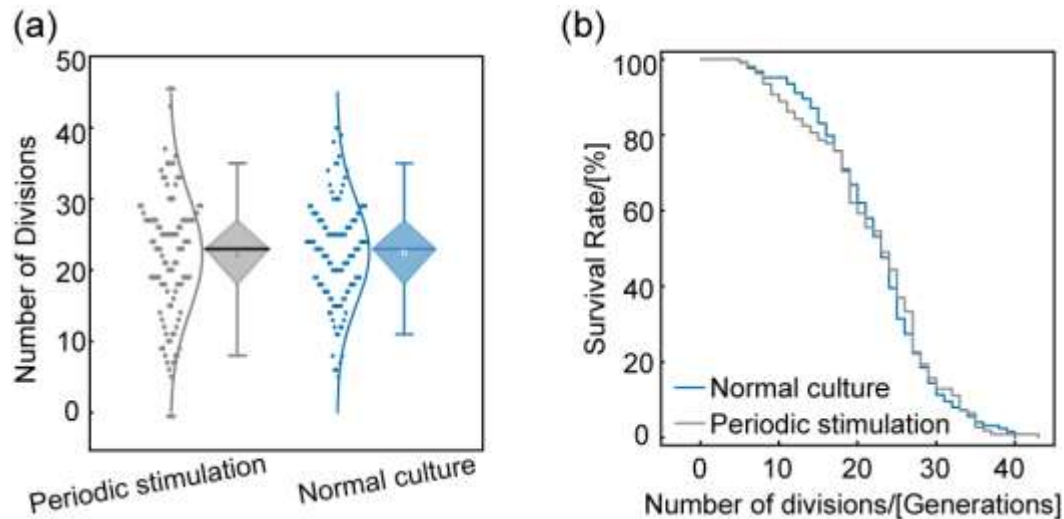
respectively.

23

24

25

26



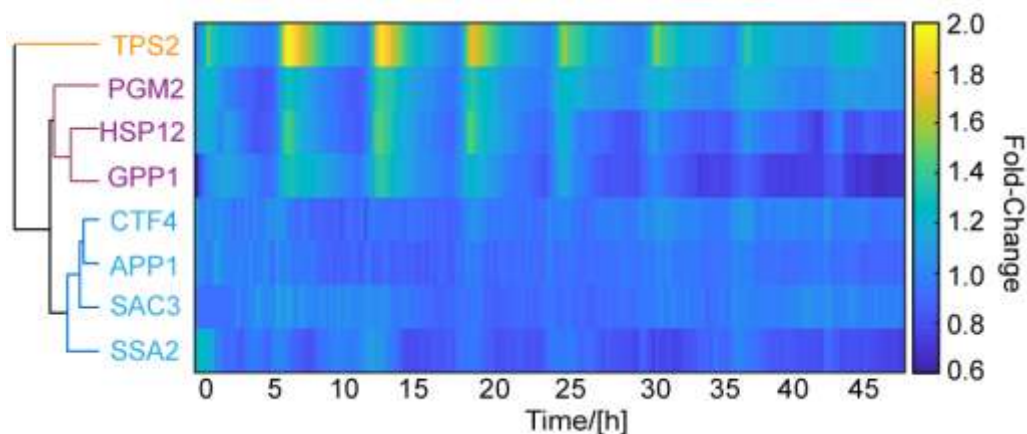
27
28
29
30
31
32
33
34
35
36
37
38
39
40
41
42
43
44
45
46
47
48
49
50
51
52
53
54
55
56
57
58

Supplementary Figure 2. Periodic mild osmotic stimulation (0.4 M KCl) does not affect the replicative lifespan of yeast cells.

(a) The lifespan distribution of yeast cells under normal culture and periodic stimulation conditions. The lifespan under both conditions showed a normal distribution, which is similar to previous conclusions obtained by using manual methods (N=124 and 108 under normal culture and periodic stimulation, respectively).

(b) Survival curves of yeast cells under two culture conditions. The replicative lifespan assay shows that compared to the normally cultured strain, strains that received the indicated stimulus exhibited a slight decrease in the mean number of generations.

59



60

61 **Supplementary Figure 3** Heat map depicts representative fold changes in the protein expression of
62 **components of the HOG1-MAPK pathway and housekeeping genes.**

63 The colored bar represents the fold change in protein expression. Different categories are indicated with different
64 colors. Osmotic-related proteins are marked in orange and purple, and the proteins independent of osmotic stress
65 are in cyan.

66

67

68

69

70

71

72

73

74

75

76

77

78

79

80

81

82

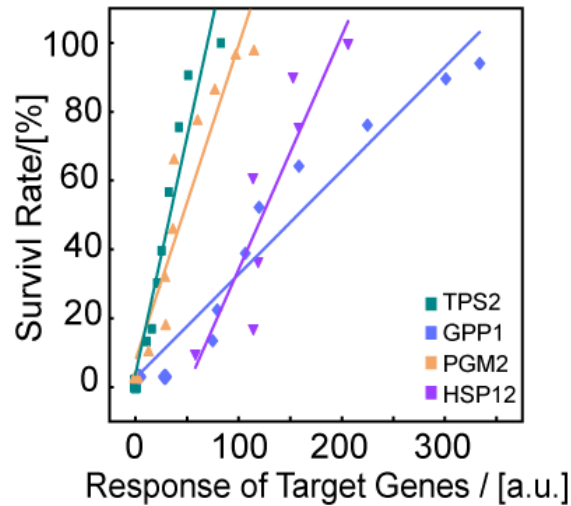
83

84

85

86

87



88

89

90 **Supplementary Figure 4. Correlation analysis revealed a linear correlation between**
 91 **averaged stress responses.**

92 For the four osmotic-related proteins, we performed a correlation analysis of the descending
 93 segments of the response curve and the survival curve. Correlation analysis revealed a linear
 94 correlation of higher than 80% on average between stress response and survival rate with the
 95 highest correlation coefficient of 93% in TPS2.

96

97

98

99

100

101

102

103

104

105

106

107

108

109

110

111

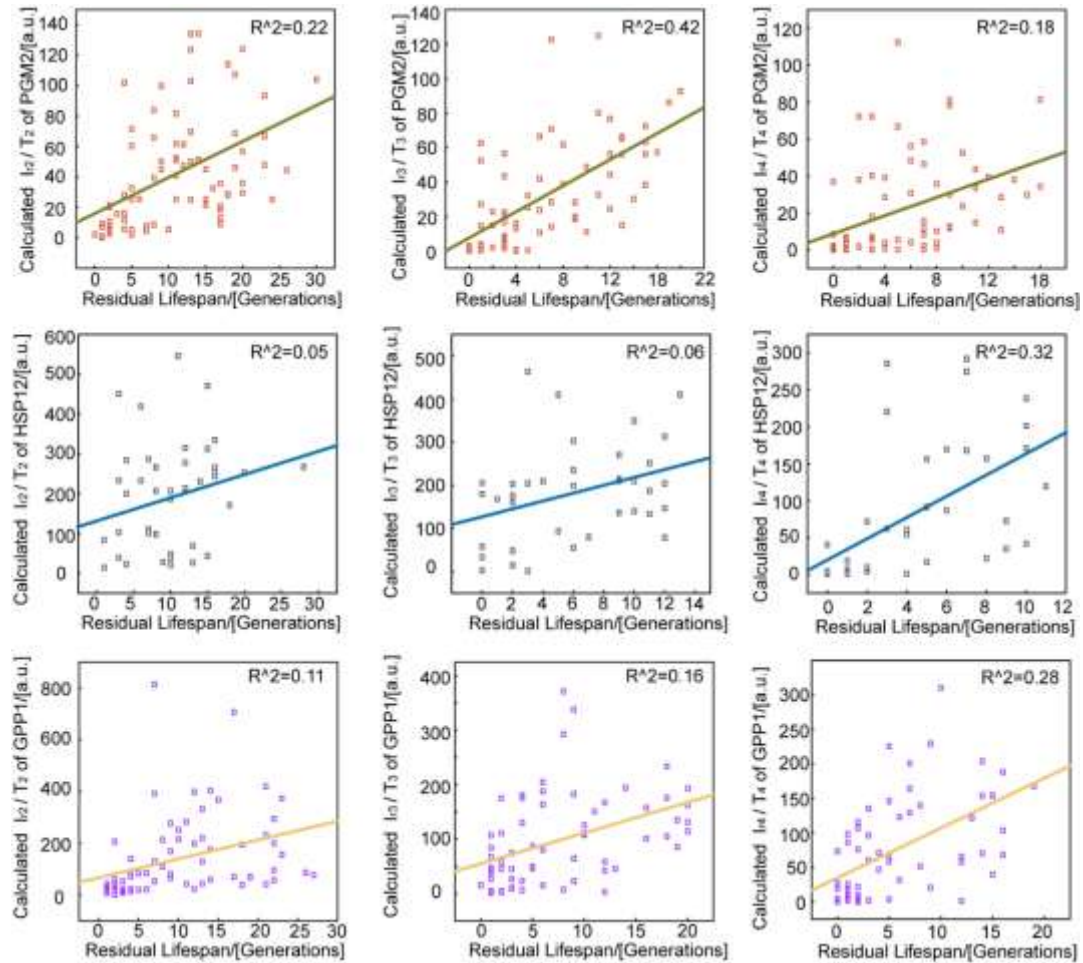
112

113

114

115

116



117

118

119 **Supplementary Figure 5. Lifespan predictability of osmotic-related proteins.**

120 We analyzed the relationship between the response capability of the four proteins to a single
 121 stimulus and the residual lifespan. Consistent with clustering results, TPS2 has the best lifespan in
 122 single-cell level ($R^2=0.58$, Fig. 4a), followed by PGM2 ($R^2=0.42$).

123

124

125

126

127

128

129

130

131

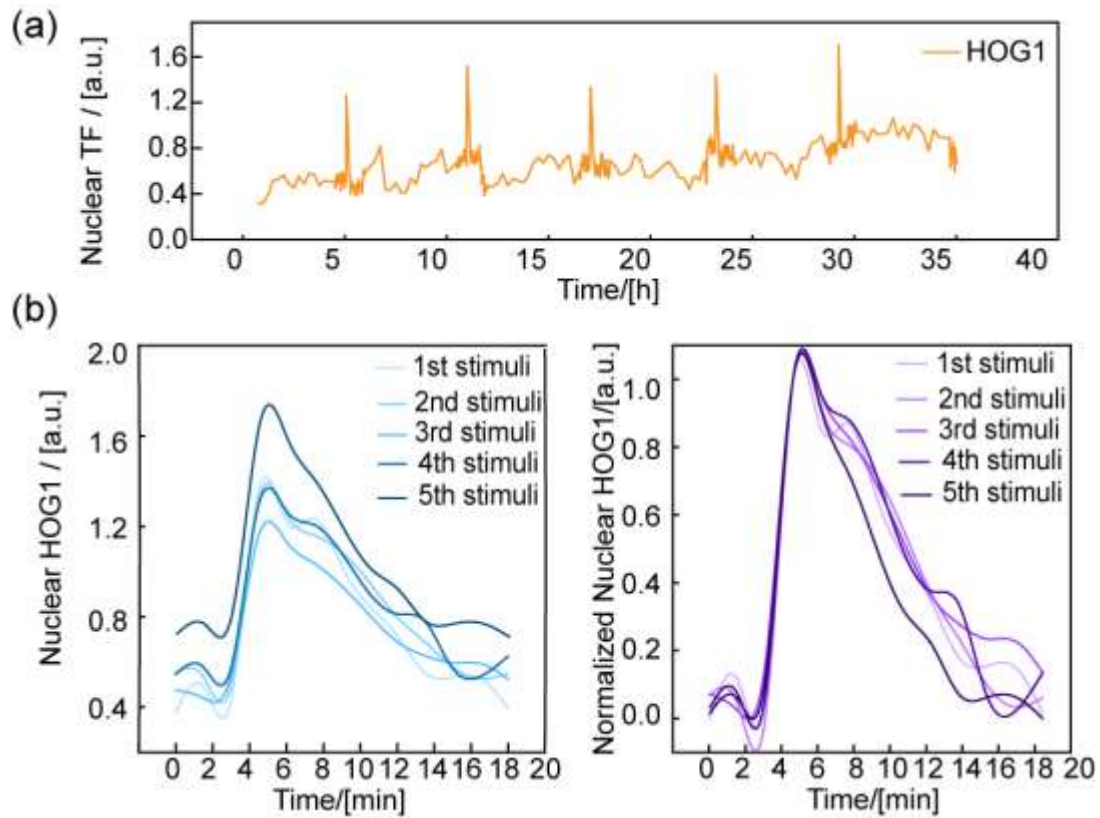
132

133

134

135

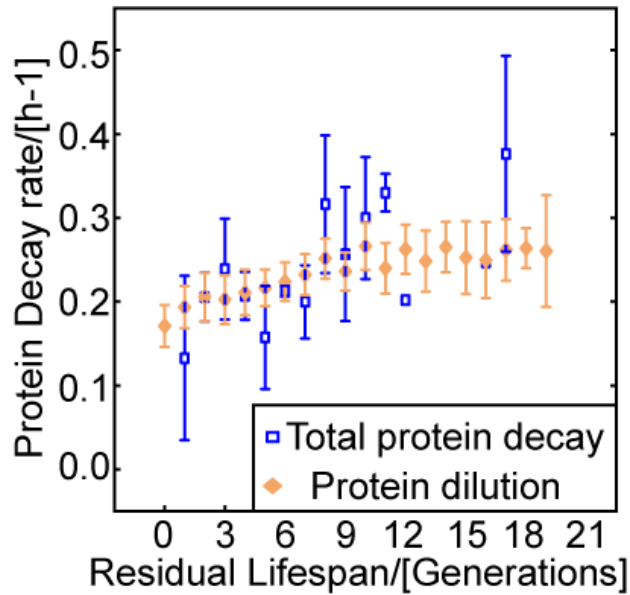
136



137
 138
 139
 140
 141
 142
 143
 144
 145
 146
 147
 148
 149
 150
 151
 152
 153
 154
 155
 156
 157
 158
 159

Supplementary Figure 6. Nuclear localization and duration analysis during aging at the single-cell level.

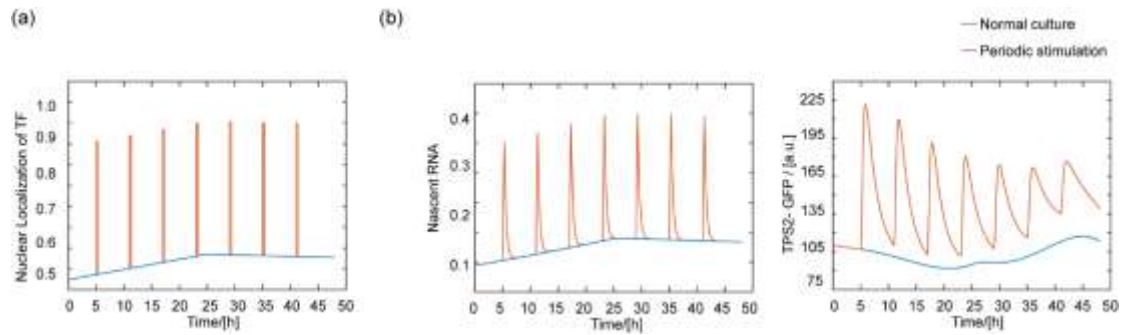
For single-cell data as an example (a), the fluorescent intensity and normalized nuclear HOG1 was demonstrated at each administered stimulation (b).



160
 161
 162
 163
 164
 165
 166
 167
 168
 169
 170
 171
 172
 173
 174
 175
 176
 177
 178
 179
 180
 181
 182
 183
 184
 185
 186
 187

Supplementary Figure 7. Dynamic changes in protein dilution and degradation during the aging process.

We used single-cell data for parameter fitting to obtain the relationship between the decay coefficient of the target protein d_2 and residual generations ($N=39$). According to Equation (6), we quantitatively measured the protein dilution caused by cell division. Through the above analysis, we deduced the effect of molecular degradation on the remaining lifespan. Although the single-cell data are relatively messy, the degradation ability of the cells was significantly reduced in the generations before death.



188
 189
 190
 191
 192
 193
 194
 195
 196
 197
 198
 199
 200
 201
 202
 203
 204
 205
 206
 207
 208
 209
 210
 211
 212
 213
 214
 215
 216
 217
 218
 219
 220
 221
 222
 223

Supplementary Figure 8. Simulated time traces of mRNA and protein from different TF inputs.

(a) curve fitting of averaged transcription factor(TF) localization time trace throughout the whole lifespan.

(b) Simulations of mRNA and downstream protein expression in response to two different transcription factor(TF) inputs (orange solid line: periodic stimulation; blue solid line: normal culture).

224 **Supplementary Table 1. Performance comparison of different abundance**
 225 **proteins.**

	TPS2	PGM2	HSP12	GPP1	CTF4	APP1	SAC3	SSA2
copy numbers (untreated) (From Yeastgenome.org)	15818	40334	42197	221168	5044	1530	1677	411582
copy numbers (under stress) (From Yeastgenome.org)	31452	66625	84487	344606	NA	NA	NA	NA
Basic fluorescent value I_0 / [a.u.](Untreated)	≈ 100	≈ 200	≈ 200	≈500	≈ 40	≈ 30	≈ 30	≈ 1000
Maximum fluorescent value under osmotic-stress I_{max} / [a.u.]	≈ 220	≈ 300	≈ 400	≈700	≈ 45	≈ 40	≈ 40	≈ 1100
Maximum synthesis rate α_{max} ([a.u.]/h)	≈ 180	≈ 220	≈ 330	≈500	≈ 35	≈ 30	≈ 30	≈ 750
Averaged synthesis rate α_0 ([a.u.]/h)	≈ 80	≈ 170	≈ 170	≈350	≈ 30	≈ 25	≈ 25	≈ 700

226

227 NA means not analysed

228 I_0 and I_{max} are the results of our experiments.

229 α_{max} and α_0 are calculated by the Euler equation¹.

230

231

232

233

234

235

236

237

238 **Computational modeling:**

239 In this phenomenological model, the binding of transcription factor immediately induces mRNA
 240 production, which then leads to the production of downstream protein². The equations describing
 241 the system as follows:

242

$$TF(t) = \begin{cases} TF_0, t > \Delta t \\ TF', 0 < t < \Delta t \end{cases}$$

$$\frac{d[mRNA]}{dt} = \frac{k_1 \cdot TF(t)^n}{K_d^n + TF(t)^n} - d_1 * [mRNA]$$

$$\frac{dP(t)}{dt} = k_2[mRNA] - d_2 * P(t)$$

243 k_1 and k_2 are the production rate of mRNA and protein; d_1 and d_2 are the mRNA and protein
 244 decay rates (degradation and dilution rate), respectively. The binding of transcription factor to
 245 DNA is governed by the Hill function, where K_d is the dissociation constant and n is the Hill

246 coefficient. Δt is the nuclear localization time of transcription factor.
 247 Then, we can get the function of mRNA $m(t)$ and protein $P(t)$ through the ODE equations.
 248

$$m(t) = \begin{cases} \frac{A}{d_1} (e^{d_1 t} - 1) e^{-d_1 t}, & 0 < t < \Delta t \\ \frac{A}{d_1} (e^{d_1 \Delta t} - 1) e^{-d_1 t}, & t > \Delta t \end{cases}$$

$$P(t) = \begin{cases} \frac{k_2 A}{d_2 - d_1} \left(\frac{1 - e^{-d_1 t}}{d_1} - \frac{1 - e^{-d_2 t}}{d_2} \right), & 0 < t < \Delta t \\ \frac{k_2 A}{d_2 - d_1} \left(\frac{e^{-d_1 t} (e^{d_1 \Delta t} - 1)}{d_1} - \frac{e^{-d_2 t} (e^{d_2 \Delta t} - 1)}{d_2} \right), & t > \Delta t \end{cases}$$

249

$$A = k_1 \left(\frac{TF'^n}{K_d^n + TF'^n} - \frac{TF_0^n}{K_d^n + TF_0^n} \right)$$

250

251

252 We fitted the averaged protein and mRNA with the function $m(t)$ and $P(t)$. The parameter sets
 253 selected from the fitting are those that gave the smallest sum of squared residual (ssq)
 254 (Supplementary Table 2).

255

256 **Supplementary Table 2. Parameter setting**

257

k_1	3.021 (h ⁻¹)
d_1	3.0 (h ⁻¹)
K_d	0.9232 (AU)
n	4
Δt	19 min

258

259 In order to verify the accuracy of the model, we fitted the time-series data of TF as input
 260 (Supplementary Fig. 8 a), and simulated the expression of mRNA and protein under given inputs
 261 (Supplementary Fig. 8 b). As shown in (Fig. 4c), the base value of transcription factors rises in the
 262 early lifespan and then flattens out, but the square pulses (above baseline) activated by osmotic
 263 stress does not change. For the two different transcription factor inputs (normal culture and
 264 periodic stimulation), the simulated protein dynamics trend is highly consistent with the
 265 experimental data.

266

267

268

269

270

271 **Reference:**

272 1. Zuleta IA, Aranda-Diaz A, Li H, El-Samad H. Dynamic characterization of growth and gene
273 expression using high-throughput automated flow cytometry. *Nat Methods* **11**, 443-448
274 (2014).

275

276 2. Hao N, O'Shea EK. Signal-dependent dynamics of transcription factor translocation controls
277 gene expression. *Nat Struct Mol Biol* **19**, 31-39 (2011).

278

279